

Electronic and crystalline structure of epitaxial EuNi_x films grown on Ni(111)

S. Wieling, S. L. Molodtsov,* and C. Laubschat

Institut für Oberflächenphysik und Mikrostrukturphysik, TU Dresden, D-01062 Dresden, Germany

G. Behr

Institut für Festkörper-und Werkstofforschung (IFW) Dresden, D-01171 Dresden, Germany

(Received 13 July 2001; published 31 January 2002)

We report on an angle-resolved and resonant photoemission study of ordered EuNi_x films grown on Ni(111). Eu is found to be trivalent in the bulk, but divalent at the surface. The low-energy electron-diffraction pattern reveals a $(\sqrt{3} \times \sqrt{3})R30^\circ$ overstructure with respect to Ni(111). Formation of a Ni-rich compound with a stoichiometry close to EuNi_5 is concluded. At the surface the stoichiometry is modified due to lattice expansion caused by the surface valence transition of the Eu ions.

DOI: 10.1103/PhysRevB.65.075415

PACS number(s): 68.35.-p, 68.55.-a, 73.20.-r

I. INTRODUCTION

In the past years electronic properties of surfaces and interfaces have become increasingly important due to the applications of thin films and nanostructures in different fields of electronics, communication, and related technologies. The broken symmetry at the surface or interface leads to the appearance of additional electronic states, electron band narrowing, and structural rearrangements, which in turn influence the magnetic coupling and may considerably change the physical and chemical properties of the systems.¹ For rare-earth (RE)-based materials, particularly large effects may be expected from changes of the $4f$ occupation n . Such phenomena known as surface valence transitions occur in Sm (Refs. 2 and 3) and Tm (Ref. 4) metals as well as in Sm-, Eu-, Tm-, and Yb-derived compounds.⁵⁻⁸ These systems are characterized by a divalent RE $[[\text{Xe}]4f^n(5d6s)^2]$ atomic configurations at the surface and a trivalent $[[\text{Xe}]4f^{n-1}(5d6s)^3]$ or mixed-valent configuration in the bulk. The valence transitions are related to the fact that for all RE's, except Ce, Gd, and Lu, the divalent configuration represents the ground state of the free atoms. The trivalent configuration is only stable if the gain in cohesive energy in the trivalent phase E_{coh}^{3+} with respect to the divalent one E_{coh}^{2+} exceeds the promotion energy U_{fd} necessary to transfer a $4f$ electron into the valence band. This condition is fulfilled for most bulk RE-based materials. At the surface, however, where cohesive energies are reduced, this condition may be violated, and the divalent configuration remains stable.^{9,10}

For heavy RE's, the $4f$ states are strongly localized and retain their atomic properties in the solids. This is particularly important for their magnetic properties, as paramagnetic moments are observed for trivalent Sm and Yb, while diamagnetic behavior is found for their divalent configurations. Thus in the case of a surface valence transition from the trivalent to the divalent configuration a diamagnetic surface layer is formed on top of a paramagnetic bulk. For Eu systems, the situation is reversed, since the trivalent $[[\text{Xe}]4f^6(5d6s)^3]$ configuration is diamagnetic while the divalent $[[\text{Xe}]4f^7(5d6s)^2]$ configuration has a large spin moment. Therefore in trivalent Eu-based compounds the unique situation may occur that a nonmagnetic bulk is termi-

nated by a magnetic surface layer. For such systems, even two-dimensional magnetic order might be achieved. A necessary condition for long-range magnetic order, however, is structural ordering, which is far from trivial for materials with surface valence transitions. In the divalent configuration, the ionic radii of the RE atoms increase by about 10% with respect to the trivalent case. This change requires strong rearrangements at the surface which may prevent the formation of an ordered surface layer. Respective surface structures have been investigated only in a few cases. In Sm metals, a (5×5) reconstruction of the divalent (0001) surface has been observed.³ The only ordered compound studied so far is EuPd_3 . Here, a (1×1) low-energy electron-diffraction (LEED) pattern was observed and a surface structure similar to EuPd_5 was concluded.¹¹

RE transition-metal compounds are particularly important due to their hard-magnetic properties. Among them multilayers of Tb and Gd with Ni are interesting as magnetic data storage materials. In this respect also Eu/Ni interfaces might be of interest since Eu^{2+} is isoelectronic to Gd^{3+} .

In the present work we report on a spectroscopic study of thin EuNi_x films grown on a Ni(111) substrate. Ordered films were grown by deposition of 80 Å Eu onto the clean Ni(111) substrate followed by annealing at 450 °C and studied by means of angle-resolved and resonant photoemission (PE) and LEED. Eu is found to be trivalent in the bulk and divalent at the surface. The formation of a compound with stoichiometry close to EuNi_5 is concluded. The surface layer of the compound is, however, strongly reconstructed due to a lattice expansion caused by the surface valence transition of the Eu atoms.

II. EXPERIMENT

A (111) surface of Ni metal was used as a substrate to grow Eu/Ni interfaces. The substrate was properly cleaned by flashing to 800 °C. Afterwards it was sputtered with Ar and annealed in O_2 atmosphere at 500 °C (5×10^{-8} mbar, 10 min). Subsequently it was annealed at 230 °C in H_2 atmosphere (5×10^{-8} mbar, 20 min). Then the Ni crystal was flashed again to 800 °C. The annealing was performed by a resistance heater mounted at the back-

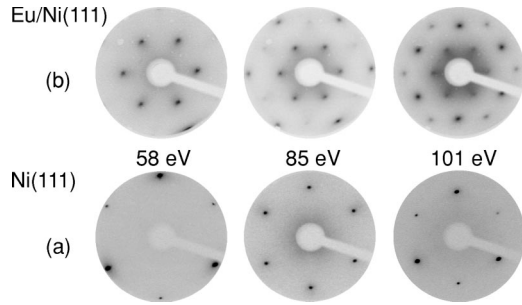


FIG. 1. LEED patterns of (a): Ni(111) and (b): Eu/Ni(111) taken at 58-, 85-, and 101-eV kinetic energies.

side of the Ni substrate. After cleaning a sharp hexagonal LEED pattern with a threefold symmetry of the spot intensities characteristic for a pure (111) surface of fcc Ni metal was observed [Fig. 1(a)]. No carbon or other bulk originating contaminations were detected with valence-band photoemission.

Eu was thermally evaporated from pellets of Eu metal inserted into a Ta crucible. In order to get rid of bulk contaminations of the evaporated material the commercially available 99.99%-clean metallic ingots of Eu (from Goodfellow, Inc.) were additionally purified by melting in Ar atmosphere and subsequent cleaning of the resulting pellets by scraping with a file. Deposition rate (about 6 Å/min) and thickness of deposited films were calibrated by means of a quartz microbalance. Deposition of 80 Å of Eu onto the Ni(111) surface resulted in a disordered interface. Structural ordering was achieved by step-by-step annealing of the interface up to a temperature of about 450 °C. The ordered interface revealed a $(\sqrt{3} \times \sqrt{3})R30^\circ$ overstructure with respect to the LEED pattern of the Ni(111) substrate. The ordered films were found to be rather nonreactive; even several hours after preparation no traces of contaminants could be detected.

Angle-resolved PE experiments on the ordered interface were performed at the Berliner Elektronenspeicherring für Synchrotronstrahlung (BESSY I) exploiting radiation from the toroidal grating monochromator beamline TGM4. Photon energies were tuned in the range from 18 to 120 eV (limit of operation of the beamline) in order to make use of energy dependent cross sections and to vary surface sensitivity in photoemission. Angle-resolved PE spectra were taken with a rotatable hemispherical electron-energy analyzer (AR65 from VSW, Inc.) with an angle resolution of 1° . Overall-system energy resolution was set to 0.25 eV [full width at a half maximum (FWHM)]. The angle between incident light and the normal to the sample surface was selected to be 50° .

A polycrystalline EuNi_5 was used as a reference sample. It was cleaned under ultrahigh vacuum conditions by scraping with a diamond file and measured with the same analyzer employing the plane grating monochromator PM 1 at BESSY II.

Resonant PE investigations were performed using the plane grating monochromator PM 5 at BESSY I, employing a Leybold-Heraeus hemispherical electron-energy analyzer with an acceptance angle of $\pm 14^\circ$ and an overall system resolution of 0.3 eV (FWHM).

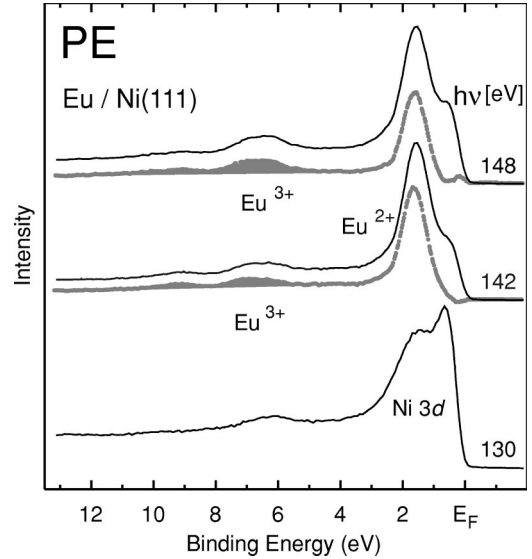


FIG. 2. Resonant PE spectra of Eu/Ni(111) taken near the resonance maxima of trivalent ($h\nu=148$ eV) and divalent ($h\nu=142$ eV) configurations and off resonance ($h\nu=130$ eV).

The base pressure in both spectrometers was in the range of 1×10^{-10} mbar.

III. Eu/Ni(111) INTERFACE

Figure 1 shows LEED patterns of the clean Ni(111) substrate (a) and the ordered surface compound (b) taken at various kinetic energies. The ordered interface reveals a $(\sqrt{3} \times \sqrt{3})R30^\circ$ overstructure with respect to the LEED pattern of the Ni(111) substrate. At 58- and 85-eV kinetic energies the intensity of the overstructure-derived LEED spots is larger than the one of the (1×1) LEED image. In contrast to the pure Ni surface, the LEED patterns reveal sixfold symmetry. A structural model will be presented further below after the discussion of the electronic and chemical properties of the compound.

In order to determine the valence of Eu in the compound, resonant PE experiments have been performed at the $4d \rightarrow 4f$ excitation threshold. Here, the $4f$ PE cross section varies dramatically due to the coupling of the direct photoionization channel with a localized $4d^{10}4f^n \rightarrow 4d^9 4f^{n+1}$ photoexcitation followed by a Super-Coster-Kronig decay. At photon energy below the threshold, $h\nu=130$ eV, the valence-band PE spectrum is expected to be almost exclusively dominated by Ni $3d$ emissions due to the destructive interference of the two excitation channels (off resonance). A corresponding off-resonance spectrum is shown at the bottom of Fig. 2. The spectrum reveals a rather narrow band with maxima at 0.7- and 1.5-eV binding energies (BE) relative to the Fermi level (E_F) and a broad satellite structure at around 6-eV BE. The latter is commonly observed in Ni systems and attributed to a $3d$ two-hole final state,^{12–15} the appearance of which may be taken as an indication that the Ni $3d$ band is not fully occupied. Above the $4d \rightarrow 4f$ threshold, first, the divalent $4f^6$ final state becomes resonantly enhanced at about 142-eV photon energy followed by the reso-

nance of the trivalent $4f^5$ emission at 148 eV.⁶ Figure 2 shows resonant PE spectra taken at 142- and 148-eV photon energies that emphasize both divalent and trivalent emissions. Since the $4f$ emissions are still superimposed by the Ni $3d$ signals, the “pure” Eu $4f$ contributions (gray thick line in Fig. 2) were extracted by subtracting the off-resonance spectrum from the on-resonance ones after normalization of the data at 0.3-eV BE. The divalent signal is obtained as a sharp peak at 1.6-eV BE corresponding to a spectroscopically unresolved 7F_6 final state, while the trivalent emissions form a broad multiplet in the region of 6-eV BE.⁶ The simultaneous appearance of both divalent and trivalent PE signals may be discussed in terms of homogeneous or inhomogeneous mixed valence: While in the former case the phenomenon is caused by configurational interaction in the ground state, in the latter case the observation of the different final states is explained by coexistence of Eu atoms with different valence at nonequivalent lattice sites. Since for a homogeneous mixed valent system the Eu $4f^6$ final state is energetically degenerated with the ground state, its binding energy is expected to be close to zero. Thus homogeneous mixed valence can be excluded in the present case on the basis of the observed large binding energy of the divalent signal.

Inhomogeneous mixed valence may be a bulk property. On the other hand, even pure trivalent bulk phases undergo usually a valence transition to the divalent configuration at the surface.^{2–6} Whether a system is mixed valent or trivalent in the bulk may be deduced from the number of divalent components in the PE spectrum: While only a single surface component is expected for a trivalent system, there should be at least two divalent components in case of a mixed-valent system, from which one arises from the bulk and the other one(s) from the surface. The energy splitting between surface and bulk components in the compound, the so-called surface core-level shift ΔE_{SCS}^{comp} , may be related to the respective shift in the pure metal ΔE_{SCS}^{met} by

$$\begin{aligned} \Delta E_{SCS}^{comp} &:= E_B^{surf} - E_B^{bulk} \cong \Delta E_{SCS}^{met} - 0.2 \cdot \Delta E_{CS}^{bulk} \\ &\cong \Delta E_{SCS}^{met} - 0.25 \cdot \Delta E_{CS}^{surf}, \end{aligned}$$

if we assume, that the chemical shift $\Delta E_{CS}^{bulk} := E_B^{bulk}(comp) - E_B^{bulk}(met)$ is reduced at the surface by 20%.¹⁶ For Eu metal, the maximum of the $4f$ -surface component is found around 2.5 eV, and ΔE_{SCS}^{met} amounts to 0.5 eV.^{17,18} Since $E_B^{surf}(comp)$ is found to be 1.6 eV in the present experiment, one obtains a E_{SCS}^{comp} value of about 0.7 eV that is large enough to be resolved spectroscopically. From the lack of a respective splitting in the PE data one may conclude that the $4f^6$ emission is due to a pure surface component and the compound behaves trivalent in the bulk. In fact, the general shape of the $4f$ emission is very close to those of other trivalent Eu compounds like EuPd_5 , that undergoes a surface valence transition.⁶ The relatively weak intensity of the trivalent bulk emission is, hereby, explained by the small mean free path of photoelectrons (about 6 Å) at these kinetic energies.

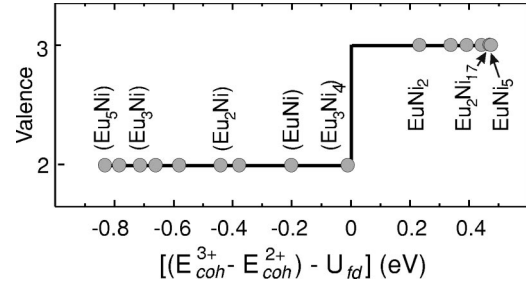


FIG. 3. Calculated valence of Eu atoms in different Eu-Ni compounds. Hypothetical compounds are lettered in brackets.

The valence of an Eu-Ni compound may be calculated by means of the semiempirical Miedema scheme.^{19–21} For compounds with more than about 60-at. % Ni concentration Eu is found to be trivalent (see Fig. 3) in agreement with experimental observations. A trivalent behavior of Eu in the bulk as concluded from the resonant PE data is therefore only compatible with the formation of a Ni-rich compound like EuNi_2 , EuNi_5 , or $\text{Eu}_2\text{Ni}_{17}$.

Within a simple tight-binding model, the width of the Ni $3d$ band is proportional to the square root of the number of nearest Ni neighbors,²² which increases with Ni concentration. Therefore the width of the valence band observed in PE experiments may be taken as a measure of the mean Ni concentration. In Fig. 4 calculated total electron densities of states (DOS) of EuNi_2 , EuNi_5 , and $\text{Eu}_2\text{Ni}_{17}$ (solid lines) are shown compared to the shape of the off-resonance PE spec-

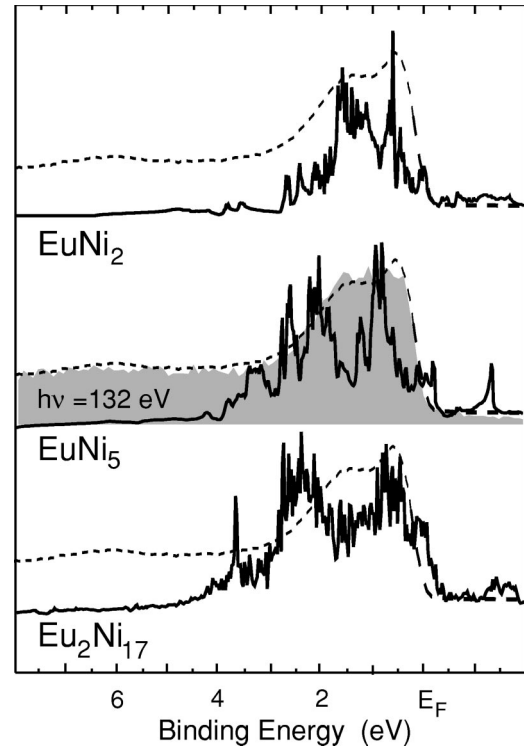


FIG. 4. Comparison between the measured off-resonance spectrum of the ordered interface (broken lines), DOS for different Eu-Ni compounds (solid lines) and the off-resonance spectrum of a polycrystalline EuNi_5 sample (shaded area).

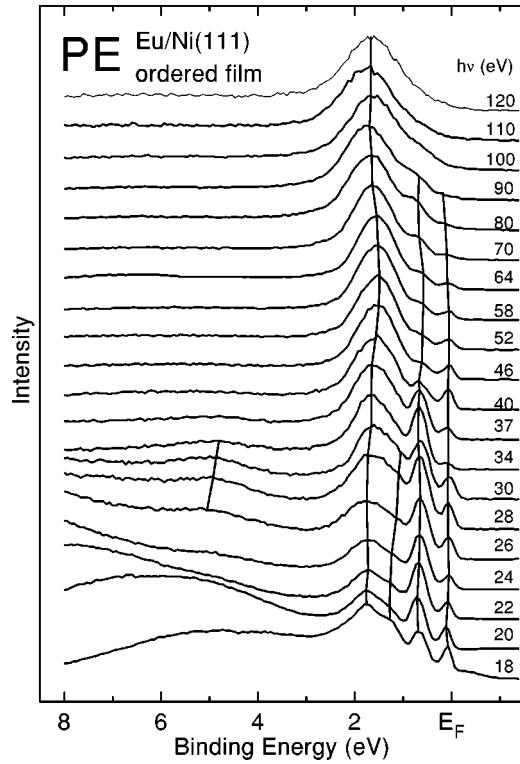


FIG. 5. Energy scan in normal emission geometry of the ordered Eu-Ni film. Spectra have been normalized to equal maximum intensity.

trum of the surface compound (dashed lines) as well as to the off-resonance spectrum of the polycrystalline EuNi_5 sample (shaded area). The calculations were performed within the local-density approximation (LDA) with the standard Hedin-Lundqvist exchange-correlation potential²³ using an optimized method of linear combination of atomic orbitals (LCAO) in its scalar-relativistic version.^{24,25} In the calculations, the compounds were handled as ideal crystals without accounting for surface and real structure effects. It should be emphasized that details of the DOS should not quantitatively be compared with angle-resolved PE data, since the latter reflect only one-dimensional optical densities of states given by discrete interband transitions. For a simple qualitative comparison, however, the similarity of the two quantities is sufficient.

The experimentally observed bandwidth and peak positions are in good agreement with the calculated DOS of EuNi_2 , while in the case of EuNi_5 and $\text{Eu}_2\text{Ni}_{17}$ the predicted large DOS around 2.5-eV BE has no counterpart in the PE spectrum. On the other hand, good agreement is observed between the off-resonant PE spectra of the film and the polycrystalline EuNi_5 sample indicating that either the band-structure calculations overestimate the bandwidth or that the photoionization cross section of the low-lying parts of the band is small. From the similarity of the spectrum of reference sample with the one of the ordered film the formation of a phase with a stoichiometry close to EuNi_5 is rather probable.

In order to get more insight into the electronic structure of the ordered film, the angle-resolved PE experiments in a

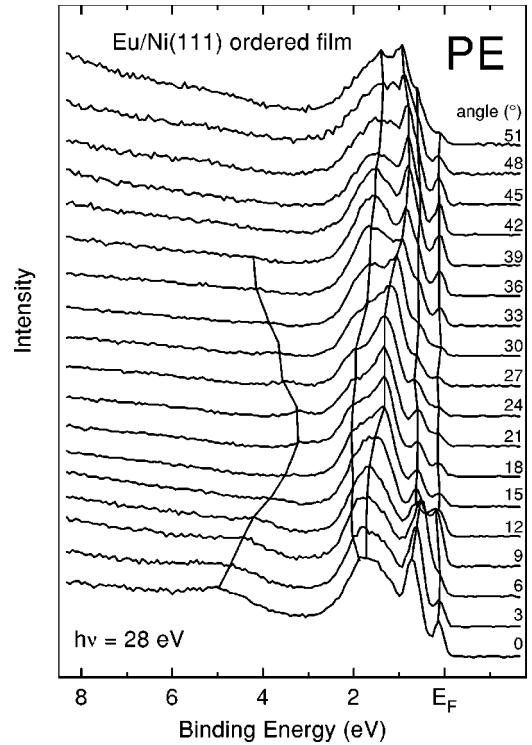


FIG. 6. Angular scan at 28-eV photon energy of the ordered Eu-Ni film. Spectra have been normalized to equal maximum intensity.

wide range of photon energies have been performed. Figure 5 shows valence-band PE spectra taken in normal emission geometry with photon energies between 18 and 120 eV. There are five features resolved in the binding energy range between E_F and 8 eV, which are marked in Fig. 5 by vertical solid lines: near E_F , around 0.7-, 1.3-, 1.7-, and 5-eV BE. The first two features are only visible up to about 90-eV photon energy, while the third one disappears already at photon energies exceeding 35 eV. The peak at 1.7 eV that dominates the spectra at photon energies above 80 eV is due to the Eu $4f^6$ signal. All other features are related to valence-band emissions. The observed dispersions are rather weak pointing to stacking faults of atomic layers perpendicular to the surface, probably related to the change of the size of Eu atoms due to the surface valence transition.

Figure 6 shows PE spectra taken at 28-eV photon energy and different polar emission angles along the $\Gamma-\bar{K}$ high symmetry direction in the surface Brillouin zone of Ni(111). In contrast to Fig. 5 the dispersion is now more pronounced. The feature near E_F vanishes at around 24° and 51° indicating a Fermi-level crossing of a band. Additional features can be seen as before at 0.7-, 1.3-, and 1.7-eV BE. The lowest-lying band is seen between 3.2-, and 5-eV BE. Both its dispersion and low intensity point to a *sp*-derived character of this feature. Obviously *d*-derived bands are restricted in energy to the first 2 eV below E_F making unlikely the formation of extremely Ni-rich compound as $\text{Eu}_2\text{Ni}_{17}$, where bandwidths around 4 eV as in Ni metal are expected (see Fig. 4).

From the electronic properties we are left with a compound composition between EuNi_2 and EuNi_5 . In fact, these

two stoichiometries are the only ones known from the bulk phase diagram in this atomic concentration regime. The Laves phase EuNi_2 does not contain lattice planes compatible with the $(\sqrt{3} \times \sqrt{3})$ -type overstructure observed in the LEED pattern of the ordered film. EuNi_5 , on the other hand, crystallizes in CaCu_5 structure and is composed of two different atomic layers, one containing only Ni and the other both Ni and Eu atoms. In the pure Ni layer of EuNi_5 , the Ni-Ni distances are increased by 1% as compared to Ni(111), and every second atom is missing in every second row leading to a (2×2) overstructure. In the other layer, the Eu atoms are located above the mentioned vacancies, whereas the Ni atoms form hexagons around the Eu sites in a way that the whole layer forms now a $(\sqrt{3} \times \sqrt{3})R30^\circ$ atomic arrangement. Since the orientation of the Eu hexagons is defined by the vacancies of the pure Ni layer, which reveals a (2×2) overstructure relative to Ni(111), the LEED pattern of a $\text{EuNi}_5(0001)$ compound is expected to be not rotated as compared to the one of the Ni substrate. Thus formation of EuNi_5 is also not in accordance with the observed LEED pattern. All other known bulk phases do not possess layers, compatible with a $(\sqrt{3} \times \sqrt{3})$ -type overstructure. On the other hand, one has to consider that LEED is particularly sensitive to the outermost surface layer that is strongly distorted by means of the surface valence transition of the Eu ions. The atomic volume of divalent Eu is larger by about 30% than the one of trivalent Eu making strong surface reconstructions necessary.

In order to develop a structural model based on the fcc matrix of Ni we may assume that the compound formation is simply achieved by replacing a number of Ni atoms by Eu atoms or vacancies and shifting of some other Ni atoms. For the trivalent bulk, formation of EuNi_5 would be in accordance with such a mechanism. Starting from a close-packed Ni layer at the Ni(111) surface, EuNi_5 may be formed by removing every second atom in every second row of the substrate. Eu atoms will be placed on the top of the resulting vacancies and the space between the rare earth will be filled by Ni atoms. For the divalent surface the same model may be applied: Starting from bulk EuNi_5 terminated by a close-packed Ni layer a $(\sqrt{3} \times \sqrt{3})R30^\circ$ overstructure may be formed at the surface by substituting every third atom from each Ni row by Eu [see Figs. 7(a) and (b)]. This corresponds to the atomic arrangement of the Eu-Ni layer in EuNi_5 , in contrast to the latter, however, the proposed structure is not rotated with respect to the Ni layers. Since the divalent Eu atoms will not fit into the Ni vacancies due to their large atomic radii, a relaxation perpendicular to the surface may be expected. Such a relaxation would be accompanied by formation of a large surface dipole layer [see Fig. 7(c)]. Since this is energetically not favorable, the space between the relaxed divalent Eu atoms could be filled by additional Ni

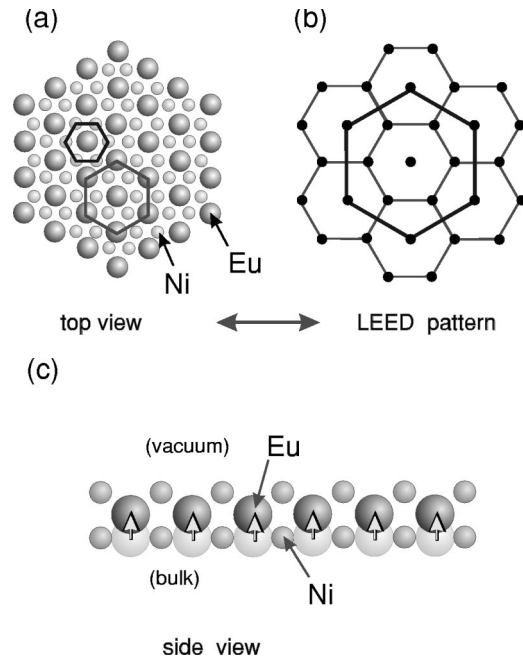


FIG. 7. Suggested surface arrangement [top (a) and side (c) view] and simulated LEED pattern (b). There is a correspondence between structures marked by hexagons of the same color (black and gray) in the real (a) and the reciprocal (b) space.

atoms. This assumption would be consistent with the observed low chemical reactivity of the ordered surface as well as with the LEED pattern.

IV. CONCLUSION

Deposition of 80-Å Eu onto a clean Ni(111) surface followed by annealing at 450 °C leads to an ordered surface compound characterized by the LEED pattern with a $(\sqrt{3} \times \sqrt{3})R30^\circ$ overstructure with respect to that of the Ni substrate. Eu is found to be trivalent in the bulk and divalent at the surface. From the PE and LEED data formation of a compound with a stoichiometry close to EuNi_5 is concluded, where the surface is heavily reconstructed due to the volume changes caused by the surface valence transition of the Eu ions.

ACKNOWLEDGMENTS

This work was supported by the Bundesministerium für Bildung und Forschung, Project No. 05Sf80D1 4, and by the Deutsche Forschungsgemeinschaft, Sonderforschungsbereich 463, TPA1 and TPB4. Technical assistance by the staff of BESSY and the group of G. Kaindl (FU Berlin) is gratefully acknowledged.

*On leave from Institute of Physics, St. Petersburg State University, 198904 St. Petersburg, Russia.

¹H. Lüth, *Surfaces and Interfaces of Solid Materials*, 3rd ed. (Springer-Verlag, Berlin, 1995).

²G.K. Wertheim and G. Creclius, *Phys. Rev. Lett.* **40**, 813 (1978).

³A. Stenborg, J.N. Andersen, O. Björneholm, A. Nilsson, and N. Mårtensson, *Phys. Rev. Lett.* **63**, 187 (1989).

⁴M. Domke, C. Laubschat, M. Prietsch, T. Mandel, G. Kaindl, and W.D. Schneider, *Phys. Rev. Lett.* **56**, 1287 (1986).

⁵C. Laubschat, G. Kaindl, W.-D. Schneider, B. Reihl, and N.

- Mårtensson, Phys. Rev. B **33**, 6675 (1985).
- ⁶W.D. Schneider, C. Laubschat, G. Kalkowski, J. Haase, and A. Puschmann, Phys. Rev. B **28**, 2017 (1983).
- ⁷G. Kaindl, C. Laubschat, B. Reihl, R.A. Pollak, N. Mårtensson, F. Holtzberg, and D.E. Eastman, Phys. Rev. B **26**, 1713 (1982).
- ⁸M. Domke, C. Laubschat, E.V. Sampathkumaran, M. Prietsch, T. Mandel, G. Kaindl, and H.U. Middelmann, Phys. Rev. B **32**, 8002 (1985).
- ⁹B. Johansson, Phys. Rev. B **20**, 1315 (1979).
- ¹⁰B. Johansson, Phys. Rev. B **19**, 6615 (1979).
- ¹¹S. Wieling, S.L. Molodtsov, T. Gantz, M. Richter, and C. Laubschat, Phys. Rev. B **58**, 13 219 (1998).
- ¹²D.R. Penn, Phys. Rev. Lett. **42**, 921 (1979).
- ¹³A. Liebsch, Phys. Rev. Lett. **43**, 1431 (1979).
- ¹⁴W. Eberhardt and E.W. Plummer, Phys. Rev. B **21**, 3245 (1980).
- ¹⁵N. Mårtensson and B. Johansson, Phys. Rev. Lett. **45**, 482 (1980).
- ¹⁶S. Wieling, S.L. Molodtsov, T. Gantz, and C. Laubschat, Phys. Rev. B **64**, 125 424 (2001).
- ¹⁷G. Kaindl, A. Höhr, E. Weschke, S. Vandré, C. Schüßler-Langeheine, and C. Laubschat, Phys. Rev. B **51**, 7920 (1995).
- ¹⁸R. Wahl, W. Schneider, S.L. Molodtsov, S. Danzenbächer, C. Laubschat, M. Richter, and E. Weschke, Phys. Rev. Lett. **82**, 670 (1999).
- ¹⁹A.R. Miedema, R. Boom, and F.R. de Boer, J. Less-Common Met. **41**, 283 (1975).
- ²⁰A.R. Miedema, J. Less-Common Met. **46**, 167 (1976).
- ²¹A.R. Miedema, J. Less-Common Met. **46**, 67 (1976).
- ²²J.F. van der Veen, F.J. Himpsel, and D.E. Eastman, Phys. Rev. Lett. **44**, 189 (1980).
- ²³L. Hedin and B.I. Lundqvist, J. Phys. C **4**, 2064 (1971).
- ²⁴H. Eschrig, *Optimized LCAO Method* (Springer, Berlin, 1989).
- ²⁵M. Richter and H. Eschrig, Solid State Commun. **72**, 263 (1989).